

promoting access to White Rose research papers



Universities of Leeds, Sheffield and York
<http://eprints.whiterose.ac.uk/>

This is an author produced version of a paper published in **British Journal of Radiology**

White Rose Research Online URL for this paper:

<http://eprints.whiterose.ac.uk/75447/>

Published paper:

Binks, DA, Hodgson, RJ, Ries, ME, Foster, RJ, Smye, SW, McGonagle, D and Radjenovic, A (2013) *Quantitative parametric MRI of articular cartilage: a review of progress and open challenges*. British Journal of Radiology, 86 (1023). 20120163

<http://dx.doi.org/10.1259/bjr.20120163>

Quantitative parametric magnetic resonance imaging of articular cartilage: a review of progress and open challenges

Short title: *Quantitative parametric MRI of articular cartilage*

Review Article

^{1,2}DA Binks, PhD, ²RJ Hodgson, PhD, FRCR, ³ME Ries, PhD, ^{1,2}RJ Foster, PhD, ^{2,4}SW Smye, PhD, ^{1,2}D
McGonagle, PhD, FRCPI, ^{*1,2}A Radjenovic, PhD

¹ Section of Musculoskeletal Disease, Leeds Institute of Molecular Medicine, University of Leeds, UK, LS2 9JT

² National Institute for Health Research, Leeds Musculoskeletal Biomedical Research Unit, Chapel Allerton Hospital, University of Leeds, UK,
LS4 7SA

³ Polymer and Complex Fluids Group, School of Physics and Astronomy, University of Leeds, UK, LS2 9JT

⁴ Academic Division of Medical Physics, University of Leeds, Leeds, UK, LS2 9JT

E-mail addresses: d.a.binks@leeds.ac.uk, richardhodgson@btinternet.com, m.e.ries@leeds.ac.uk, r.j.foster@leeds.ac.uk,
s.w.smye@leeds.ac.uk, d.g.mcgonagle@leeds.ac.uk, a.radjenovic@leeds.ac.uk

**Corresponding Author*

This work was funded through WELMEC, a Centre of Excellence in Medical Engineering funded by
the Wellcome Trust and EPSRC, under grant number WT 088908/Z/09/Z.

**Quantitative parametric magnetic resonance imaging of articular cartilage: a review of
progress and open challenges**

Review Article

1
2
3
4
5
6
7
8
9
10
11
12
13
14
15
16
17
18
19
20
21
22
23
24
25
26
27
28
29
30
31
32
33
34
35
36
37
38
39
40
41
42
43
44
45
46
47
48
49
50
51
52
53
54
55
56
57
58
59
60
61
62
63
64
65

1
2
3
4 **Abstract**
5

6 *With increasing life expectancies and the desire to maintain active life-styles well into old age, the*
7 *impact of the debilitating disease osteoarthritis (OA) and its burden on health care services is*
8 *mounting. Emerging regenerative therapies could deliver significant advances in the effective*
9 *treatment of OA but rely upon the ability to identify the initial signs of tissue damage and will also*
10 *benefit from quantitative assessment of tissue repair in vivo. Continued development in the field of*
11 *quantitative magnetic resonance imaging (MRI) in recent years has seen the emergence of*
12 *techniques able to probe the earliest biochemical changes linked with the onset of OA. Quantitative*
13 *MRI measurements including T_1 , T_2 and $T_{1\rho}$ relaxometry, diffusion weighted imaging and magnetisation*
14 *transfer have been studied and linked to the macromolecular structure of cartilage. Delayed*
15 *gadolinium-enhanced MRI of cartilage (dGEMRIC), sodium MRI and glycosaminoglycan chemical*
16 *exchange saturation transfer (gagCEST) techniques are sensitive to depletion of cartilage*
17 *glycosaminoglycans (GAG) and may allow detection of the earliest stages of OA. We review these*
18 *current and emerging techniques for the diagnosis of early OA and evaluate the progress that has*
19 *been made towards their implementation in the clinic and identify future challenges in the field.*
20
21
22
23
24
25
26
27
28
29
30
31
32
33
34
35
36
37
38
39
40
41
42
43
44
45
46
47
48
49
50
51
52
53
54
55
56
57
58
59
60
61
62
63
64
65

1
2
3 **Introduction**

4 The treatment of the degenerative joint disease osteoarthritis (OA) remains problematic. For
5 advanced end stage “whole organ” disease the only viable treatment option is joint replacement
6 where feasible. For earlier stage OA, disease progression is unpredictable and often slow which
7 makes it very difficult to evaluate agents that have possible disease modifying properties. Although
8 the OA disease process may commence within any joint structure including ligaments, bone,
9 meniscus or articular cartilage, the advancement of disease is inevitably associated with progressive
10 cartilage attrition and inexorable functional deterioration. The non-invasive assessment of tissue
11 damage (at a stage in the disease process where tissue damage is potentially reversible) and the
12 ability to monitor its repair during and following treatment is central to future development of novel
13 therapies aimed at arresting or reversing cartilage destruction.
14
15
16
17
18
19
20
21
22
23
24
25

26 The purpose of this review is to evaluate current and emerging quantitative magnetic resonance (MR)
27 protocols for assessment of cartilage in order to identify the open challenges that will drive further
28 development in the field. Of specific interest are the methods that can detect the initial stages of
29 cartilage degradation and also those that allow the biomechanical properties of cartilage to be
30 studied. Such techniques might be important aids for early diagnosis of arthritic diseases and also in
31 assessing the progress of regenerative and reparative therapies for OA *in vivo*. [1, 2] An ideal scenario
32 would be the development of high resolution whole body magnetic resonance imaging methods that
33 could provide functional information about the state of cartilage at multiple sites, in a timely and cost
34 effective fashion, without resort to exogenous contrast agents. This is particularly challenging for the
35 assessment of cartilage as high spatial resolution is required. We will discuss what degree of
36 progress has been made towards that lofty goal where MRI biomarkers could be used to reliably
37 identify and characterise early cartilage damage or sites at risk of cartilage loss.
38
39
40
41
42
43
44
45
46
47
48
49
50
51
52
53

54 **Cartilage composition**

55 The purpose of articular cartilage is to provide a wear-resistant, low friction, force distributing material
56 between the comparatively rigid subchondral bone surfaces in diarthrodial joints. At a macromolecular
57 level cartilage consists of an extracellular matrix (ECM) made up of a network of collagen fibrils and
58
59
60
61
62
63
64
65

1 proteoglycan (PG) molecules.[3] PG itself consists of a protein core with covalently attached
2 negatively-charged glycosaminoglycans (GAGs). This macromolecular matrix accounts for around 20-
3 30% of the tissue weight. The rest is made up of fluid, containing mobile charge-balancing cationic
4 species[4] (Figure 1a). The mechanisms by which the electrolytic fluid, collagen network and
5 proteoglycan interact with each other confer articular cartilage its biomechanical properties and allow
6 it to withstand and distribute the various forces experienced during joint articulation. Early
7 osteoarthritic changes in articular cartilage occur in the ECM with loss of proteoglycan accompanied
8 by heightened water content.[5] The loss of proteoglycan and, therefore, negative fixed charge
9 density (FCD) results in increased water mobility in the cartilage matrix and a diminished capacity to
10 cope with mechanical loading (Figure 1b). This in turn exposes the cartilage to further degradation.
11 Thus there is a great deal of interest and merit in searching for diagnostic techniques that are
12 sensitive to the earliest micro-scale biochemical changes associated with cartilage degradation and
13 OA.[2]

30 **MRI of cartilage**

31 Since its introduction into clinical practice in the 1980s, MRI has become a powerful and capable
32 diagnostic tool, and excels in its ability to acquire images with a high degree of soft-tissue contrast
33 non-invasively and in 3-D.[6] Image contrast can be varied through choice of imaging parameters in
34 order to emphasise different types of tissue. In conventional MRI sequences contrast is typically
35 afforded by making the signal intensity of each pixel in the image partially dependent upon – or
36 “weighted” by – either the T_1 or T_2 relaxation time of the hydrogen nuclei contained within that pixel.
37 The T_1 and T_2 relaxation times of nuclei are determined by their physiochemical environment and can
38 thus vary between different tissue types. MR sequences in which both T_1 and T_2 weighting are
39 minimized are said to be proton density weighted, meaning the signal is determined almost solely by
40 the local concentration of hydrogen nuclei.
41
42
43
44
45
46
47
48
49
50
51

52 MRI is already widely used in the clinic for assessment of articular cartilage and gross joint
53 morphology as well as the identification of other arthritic features including osteophytes, bone marrow
54 oedema and meniscal and ligament tears.[7-10] The need to differentiate between articular cartilage
55
56
57
58
59
60
61

1 and a range of surrounding tissue types (bone, muscle, fat, synovial fluid *etc.*), has meant that a
2 number of MR pulse sequences are used in a typical clinical assessment (Figure 2). The design of the
3 National Institute of Health Osteoarthritis Initiative knee MRI protocol[7] serves to highlight the variety
4 of sequences implemented; the protocol includes sequences with T_1 -weighted, T_2 -weighted and
5 intermediate-weighted contrasts utilising both spin-echo (SE) and gradient recalled echo (GRE)
6 methods. Imaging planes are prescribed in sagittal and coronal directions and 2-D and 3-D images
7 are acquired with the latter allowing for images to be reconstructed in multiple planes. The entire
8 protocol is designed to be performed in a relatively short timeframe with respect to patient comfort
9 and allows quantitative and semi-quantitative assessments of a multitude of structural features and
10 pathologies within the knee joint.
11
12
13
14
15
16
17
18
19
20
21
22
23

24 Advances in the design of superconducting magnets have facilitated scanners and spectrometers with
25 stronger static magnetic fields, allowing for imaging with a combination of increased signal-to-noise
26 ratio (SNR), higher spatial resolution and accelerated acquisition time. Experimental narrow-bore
27 magnets with field strengths of 9.4 T and 11.7 T are common, whilst whole body scanners with 3.0 T
28 fields are becoming more prevalent in clinical settings.[11] Similarly, progress in imaging pulse
29 sequence design and development of more sensitive and sophisticated radiofrequency (RF) coils has
30 led to MRI techniques that are able to directly assess the microscopic structure and biochemical
31 composition of musculoskeletal tissues in addition to imaging macroscopic structural and anatomical
32 detail. The capacity to determine microscopic structure and composition is a key factor for diagnosis
33 of OA as macroscopic degenerative changes (*e.g.* cartilage defects or joint space narrowing) are
34 usually absent in the early stages of the disease.[12] Moreover, gross structural changes with joint
35 malalignment may not be amenable to putative therapies.[13] The remainder of this review will focus
36 on emergent quantitative MRI techniques that allow this microscopic assessment of articular cartilage.
37
38
39
40
41
42
43
44
45
46
47
48
49
50
51
52
53

54 **T_1 relaxation**

55 Whereas signal intensity in the weighted imaging sequences briefly introduced above is a function of
56 both the concentration (spin-density) and one or more intrinsic properties (*e.g.* T_1 , T_2) of the imaged
57
58
59
60
61
62
63
64
65

1 nuclei, the aim with quantitative MRI techniques is to survey or “map” the absolute value of these
2 intrinsic properties on a pixel-by-pixel basis (Figure 3).
3

4 The spin-lattice or T_1 relaxation time governs the rate at which nuclei return energy to their
5 surroundings (the “lattice”) following excitation.[14] The factors affecting native T_1 relaxation times in
6 articular cartilage are not well understood though it has been reported that native T_1 values are
7 sensitive to the macromolecular structure of the cartilage matrix.[15] The exact nature of this
8 relationship is unclear, but is believed to relate more to the PG content of the tissue than the collagen
9 architecture.[16] A systematic survey of native T_1 in different cartilage compartments of healthy
10 human volunteers was undertaken by Wiener *et al.*[17] In this study, T_1 values were shown to
11 decrease from the superficial cartilage layers to the deep layer, consistent with the dependence of
12 native T_1 values upon the macromolecular construction of cartilage.
13
14
15
16
17
18
19
20
21
22
23
24
25
26

27 **Contrast enhanced T_1 - dGEMRIC**

28 The studies described in the previous section are primarily concerned with the native T_1 relaxation
29 time of cartilage. An area which has received considerably more attention is the mapping of the T_1
30 relaxation time of cartilage in the presence of the gadolinium contrast agent gadolinium
31 diethylenetriamine pentaacetic acid ($[\text{Gd}(\text{DTPA})^2]$). This forms the basis of the delayed gadolinium-
32 enhanced MRI of cartilage (dGEMRIC) technique.[18] The distribution of the negatively-charged
33 contrast agent is inversely proportional to the cartilage fixed charge density due to the presence of
34 negatively-charged GAG side chains on proteoglycan (Figure 4). Areas of cartilage with depleted
35 GAG concentration therefore accumulate more contrast agent. The highly paramagnetic gadolinium
36 ions promote relaxation processes, leading to a localised reduction in the T_1 relaxation time.
37 dGEMRIC can, therefore, be used to determine the spatial variation of tissue GAG concentration and
38 is a technique that shows promise as a specific measure of early degradation in the cartilage ECM
39 associated with OA.[19] In a clinical setting, there is support for the efficacy of the technique for
40 detecting pre-radiographic signs of OA in the knee[20] and hip joints[21].
41
42
43
44
45
46
47
48
49
50
51
52
53
54
55

56 A number of practical considerations relating to the *in vivo* implementation of the dGEMRIC technique
57 have been investigated and addressed by Burstein *et al.*[22] The relationship between the contrast
58 enhanced T_1 and GAG concentration is subject to effective penetration of the contrast agent into the
59
60
61
62
63
64
65

1 cartilage, which may be affected by a patient's body mass index (BMI) and/or ratio of fat to lean
2 tissue. They recommend intravenous injection of a double dose (0.2 mM kg^{-1}) of $\text{Gd}(\text{DTPA})^{2-}$, followed
3
4 by a 10 minute period of exercising the joint to aid penetration of the contrast agent into the cartilage.
5
6 Maximum contrast is achieved 2 hours post injection for the knee joint. A separate study reports that
7
8 complete equilibration of $[\text{Gd}(\text{DTPA})^{2-}]$ throughout the entire thickness of the cartilage may take as
9
10 long as 12 hours.[23] Additionally, the direction and type of loading experienced by the joint during the
11
12 exercise period may affect the distribution of the contrast agent.[24]
13

14
15 A further consideration for dGEMRIC is whether both pre- and post-contrast T_1 values are required to
16
17 accurately evaluate variations in cartilage GAG content.[1, 25-27] Where only the post-contrast T_1 is
18
19 used to report the so called dGEMRIC index, the assumption has been made that the pre-contrast
20
21 value of T_1 (T_{1_0}) is relatively constant and that the post-contrast value of T_1 is sufficiently small
22
23 compared to T_{1_0} . The current consensus is that the post-contrast T_1 gives a sufficiently accurate
24
25 measure of GAG concentration and the time-consuming measurement of pre-contrast T_1 is not
26
27 necessary.[28]
28
29

30
31 Apart from these concerns, there is a desire to implement faster T_1 mapping protocols with higher
32
33 resolution and 3-D joint coverage. This would be beneficial for both *in vitro* and *in vivo* studies alike
34
35 because quantitative T_1 mapping techniques are typically time consuming. This is increasingly
36
37 relevant at higher field strengths where T_1 relaxation times increase, resulting in even longer scan
38
39 times.[29] Accurate 3-D T_1 mapping protocols have been implemented on 1.5 T and 3.0 T platforms
40
41 using 3-D inversion recovery spoiled gradient echo,[29] 3-D Look-Locker[30] and 3-D fast two-angle
42
43 T_1 mapping[31] methods.
44
45
46
47

48 **T_2 relaxation**

49
50 T_2 relaxation concerns the loss of phase coherence between nuclei following excitation by an RF
51
52 pulse. Immediately after the excitation, nuclei have phase coherence resulting in a detectable net
53
54 magnetisation vector.[14] As T_2 relaxation occurs, this phase coherence is lost and the observable
55
56 NMR signal decays exponentially with time. In cartilage, the restricted motion of water molecules
57
58 imposed by the macromolecular structure of the ECM promotes relaxation, resulting in shorter T_2
59
60
61
62
63
64
65

1 relaxation times.[1] T_2 relaxation times are therefore dependent on both the water content and
2 condition of the surrounding macromolecular structure.[32] Increased hydration of cartilage and
3 breakdown of cartilage collagen are both early indicators of osteoarthritic disease[5] and as such
4 there is considerable interest in the potential for T_2 to be used as a predictor of early OA.[33] Early
5 work in this area was conducted by Dardzinski et al in a study of 7 asymptomatic adults.[34] Cartilage
6 T_2 relaxation times were shown to vary across the thickness of the cartilage in a manner consistent
7 with the known spatial distribution of cartilage water and proteoglycan content. The erosion of the
8 cartilage ECM and increased tissue water content associated with degraded tissue is generally linked
9 with higher T_2 values. Dunn *et al* have reported on the correlation between increased T_2 values and
10 severity of OA in a study of 55 patients.[35]. Subjects with mild and severe OA had significantly higher
11 cartilage T_2 values than healthy subjects. A study of the Osteoarthritis Initiative patient cohort has also
12 shown a link between heightened T_2 values of patellar cartilage and knee abnormalities.[36] It has,
13 however, been suggested[1] that explicit interpretation of changes in T_2 should be made with care,
14 due to the number of competing biological and mechanical effects that influence T_2 .

15
16
17
18
19
20
21
22
23
24
25
26
27
28
29 The effect of the collagenous architecture on T_2 relaxation times is evident in the zonal variation of T_2
30 values in the deepest cartilage layers adjacent to the bone and in the tangential zone cartilage at the
31 articular surface. In the deep and tangential layers of articular cartilage where the orientation of
32 collagen fibrils is anisotropic, T_2 values show a dependence on the alignment of the cartilage with the
33 static magnetic (B_0) field.[37, 38] This dependence is not observed in the intermediate cartilage layer
34 where there is a random distribution of collagen fibril orientations. The effect on T_2 values arises due
35 to the so called magic angle effect[14] whereby the dipole-dipole interactions between nuclei that
36 promote relaxation are minimised when the angle between the inter-nuclear vector and the static
37 magnetic field is 54.7° . While it is apparent that T_2 values in cartilage are strongly influenced by the
38 collagen architecture, with a study by Nissi *et al*[39] suggesting 60% of the variation in T_2 values can
39 be rationalised by changes in the collagen fibril orientation, the remaining 40% is then determined by
40 other factors including water content[40] and concentration of other macromolecules.[41] This
41 reiterates the need for care in interpreting variation in T_2 relaxation times.

42
43
44
45
46
47
48
49
50
51
52
53
54
55
56
57
58
59
60
61
62
63
64
65
A further consideration for evaluation of cartilage T_2 relaxation times is the need for MR pulse
sequences that are able to probe tissues with short (< 10 ms) T_2 values, including calcified cartilage

1 and fibrocartilage.[42] Ultrashort echo time (UTE) MRI sequences are sensitive to these very short
2 relaxation times and allow quantitative assessment of the highly organised collagen network
3 particularly in the deep and calcified cartilage zones.[43]
4
5
6
7
8

9 **$T_{1\rho}$ relaxation**

10 The spin-lattice relaxation time in the rotating frame ($T_{1\rho}$) is sensitive to low frequency exchange
11 interactions between water molecules and the large, slow tumbling macromolecules that constitute
12 the cartilage ECM.[33] $T_{1\rho}$ measurements are performed by using a preparatory spin-locking pulse
13 that attenuates T_2 relaxation and causes the magnetisation to evolve according to the $T_{1\rho}$ relaxation
14 time of the nuclei.[44] Following the spin-locked preparation of the magnetisation, spatial encoding of
15 the NMR signal can be achieved using standard sequences, including spin echo[45] and gradient
16 echo.[46, 47] Variation of the pulse duration allows points on the $T_{1\rho}$ decay curve to be sampled and
17 the $T_{1\rho}$ relaxation time determined.
18
19
20
21
22
23
24
25
26
27

28 $T_{1\rho}$ measurements have been shown to be sensitive to changes in proteoglycan content in
29 enzymatically degraded bovine cartilage[45, 48] indicating the potential for $T_{1\rho}$ to be used as a
30 biomarker for the early stages of OA. A more recent study has examined the ability of quantitative $T_{1\rho}$
31 measurements to identify cartilage degeneration as validated by arthroscopic investigation, with $T_{1\rho}$
32 showing the potential to identify cartilage with softening and swelling corresponding to a grade I
33 classification on the Outerbridge scale used for visual assessment of chondral lesions.[49] Evaluation
34 of cartilage repair in patients undergoing microfracture and mosaicplasty surgical procedures has also
35 been performed[50] using $T_{1\rho}$.
36
37
38
39
40
41
42
43
44
45

46 There are several studies comparing the relative sensitivities of quantitative $T_{1\rho}$ and T_2 measurements
47 to the earliest degenerative changes in the cartilage ECM.[51, 52] The consensus is that $T_{1\rho}$ may be
48 more sensitive to the initial changes in the cartilage ECM associated with PG depletion whereas T_2 is
49 only sensitive to later changes in the collagen network. Furthermore, the relative change in $T_{1\rho}$ values
50 in healthy tissue versus degenerative tissue is larger than for T_2 , offering an improvement in dynamic
51 range for detecting early OA pathology.[53] It has also been shown that $T_{1\rho}$ values appear to be
52 unaffected by the laminar structure of cartilage.[54]
53
54
55
56
57
58
59
60
61
62
63
64
65

1
2
3
4
5
6
7
8
9
10
11
12
13
14
15
16
17
18
19
20
21
22
23
24
25
26
27
28
29
30
31
32
33
34
35
36
37
38
39
40
41
42
43
44
45
46
47
48
49
50
51
52
53
54
55
56
57
58
59
60
61
62
63
64
65

There are still conflicting opinions on the specificity of $T_{1\rho}$ measurements for measuring PG content[1, 44, 55] because $T_{1\rho}$ may be at least partially susceptible to the same competing factors that limit the specificity of T_2 measurements, such as tissue collagen content and hydration. The availability of standard clinical $T_{1\rho}$ pulse sequences can also be problematic.[1] Additionally, the long duration of the spin-locking pulse means that large amounts of RF energy are transmitted to the subject during the pulse sequence, and this must be controlled within prescribed limits for safe use on patients.[44] This is particularly pertinent at higher field strengths as the RF energy transmitted for any discrete excitation increases with the square of the field strength.[56]

Relationship between mechanical properties of cartilage and quantitative MRI

21
22
23
24
25
26
27
28
29
30
31
32
33
34
35
36
37
38
39
40
41
42
43
44
45
46
47
48
49
50
51
52
53
54
55
56
57
58
59
60
61
62
63
64
65

Due to the sensitivity of certain MR techniques to the macromolecular structure and content of articular cartilage, there is a related interest in the prediction of the mechanical properties of cartilage using these non-invasive MRI methods. Continued development of such methods could have a significant impact on the ability to inform biotribological studies of articular cartilage wear and degeneration.[57, 58]

Nissi *et al* have attempted to determine the relationship between the mechanical properties of human, bovine and porcine patellar cartilage and MR parameters of the tissue.[15] Native T_1 and T_2 values and the gadolinium-enhanced T_1 (dGEMRIC) were measured along with the Young's modulus and dynamic modulus of the samples. Lower native T_1 relaxation times were found in tissue with high stiffness possibly reflecting the reduced water content and high concentration of collagen and PG in such areas. The relationship between stiffness and T_2 values was less clear. Differences in the laminar structure of the cartilage samples relating to the varying stages of maturity presented a complex relationship between stiffness and bulk T_2 values. However, a significant correlation was observed when data for human, bovine and porcine cartilage were pooled together. Somewhat surprisingly, given the relationship between dGEMRIC and PG content, the study did not find any significant correlation between the measured mechanical properties and contrast enhanced T_1 values. This was attributed to the dominating effect of the collagen architecture to which dGEMRIC is insensitive. Juras *et al*[59], have since reported a high correlation between contrast enhanced T_1

1 values and the instantaneous and equilibrium modulus values of human cartilage explants. This study
2 also reiterated the difficulty in correlating T_2 with stiffness values.
3

4 The sensitivity of $T_{1\rho}$ measurements to proteoglycan content has been exploited by Wheaton *et al*[60]
5 in an attempt to measure mechanical properties of cartilage using MRI. In this work, changes in the
6 $T_{1\rho}$ relaxation time were shown to correlate with both the proteoglycan content, as determined by
7 spectrophotometric assay, and the compressive modulus and hydraulic permeability of bovine
8 cartilage samples.
9

10 More recent work by the group from the University of Kuopio has involved the development of a finite
11 element model (FEM)[16, 61] to infer mechanical properties of cartilage from MR parameters and
12 other complementary methods *e.g.* infrared imaging and polarised light microscopy. This work
13 concludes that a FEM can infer mechanical properties of cartilage, given the depth-dependent
14 collagen content, the PG and water content and collagen architecture. MR techniques can determine
15 water and PG content and collagen architecture, but not the collagen content.
16
17
18
19
20
21
22
23
24
25
26
27
28
29
30

31 **Sodium-MRI**

32 Sodium-MRI offers an alternative method to dGEMRIC for the measurement of cartilage FCD.
33

34 Negative FCD in the cartilage ECM is charge balanced by the presence of positively-charged sodium
35 ions (Figure 5). Thus, determination of the concentration of sodium within the tissue allows the
36 negative FCD, and hence GAG concentration, to be quantified.[44] The first evidence of the suitability
37 of sodium MRI for this type of measurement was presented as far back as 1988.[62] Gradient echo
38 MR images of various tissues, including cartilage, were obtained at 1.9T with moderate acquisition
39 times (2-30 minutes). As with the dGEMRIC method, measurement of FCD using sodium MRI is
40 highly specific to the GAG concentration but importantly, does not require the use of a contrast agent;
41 intravenous administration of contrast agent is invasive and potentially uncomfortable for the patient,
42 prolongs the examination time and has been associated with increased risk of nephrogenic fibrosing
43 dermatopathy.[63] Several reports[64-66] have since demonstrated the specificity of the technique for
44 detecting cartilage degradation through small changes in the FCD, along with improvements in image
45 quality and speed of image acquisition. Clinical studies of cartilage using sodium-MRI remain
46
47
48
49
50
51
52
53
54
55
56
57
58
59
60
61
62
63
64
65

1 comparatively rare, hampered by the technical difficulties of obtaining sufficient signal-to-noise in a
2 clinically relevant time frame.
3

4 The major challenges involved in sodium MRI arise due to the inherently lower concentration of ^{23}Na
5 nuclei in the cartilage ECM and a smaller gyromagnetic ratio compared to the ^1H nucleus. The T_1 and
6 T_2 relaxation times of sodium are also comparably short. Combined, these factors have an impact on
7 the achievable signal-to-noise ratio and image resolution using the technique.[44] Signal loss due to
8 rapid T_2 relaxation can be offset by the use of ultrashort echo time sequences.[67] Indeed, a precise
9 measurement of sodium concentration using sodium MRI necessitates the use of UTE or similar
10 sequences due to the rapid T_2 relaxation rate of the sodium nucleus.[44] SNR enhancement is also
11 facilitated through the use of radial k -space acquisition trajectories,[68, 69] where the NMR signal is
12 acquired immediately after excitation from the centre of k -space and therefore does not undergo
13 decay during the phase-encoding steps required in a conventional Cartesian k -space trajectory.
14
15
16
17
18
19
20
21
22
23
24
25
26
27

28 **Magnetisation transfer**

29 In a conventional MR imaging sequence, it is the hydrogen nuclei of unbound bulk water molecules
30 that contribute to the observed signal. In a magnetisation transfer sequence, a preparatory saturation
31 pulse is applied prior to the main MR sequence, which excites the broad signal of less mobile
32 macromolecule-bound water molecules (Figure 6a). Exchange between the two water pools results in
33 an attenuation of the bulk water signal, the extent of which depends on the kinetics of the exchange
34 process and the volume of the bound water pool.[70] Magnetisation transfer contrast (MTC) is
35 therefore used to highlight interactions between the bulk water and macromolecules (bound water).
36 The extent of magnetisation transfer is often expressed as the magnetisation transfer ratio (MTR)
37 which is simply the ratio of signal intensities observed with and without the application of the
38 preparatory saturation pulse. An alternative metric is the rate constant for exchange of water between
39 the two pools.[71]
40
41
42
43
44
45
46
47
48
49
50
51
52
53

54 For cartilage imaging the important magnetisation transfer interaction is between bulk water and water
55 bound to the collagen fibres present in the cartilage ECM although there is also a contribution from
56 proteoglycan.[72-75] Regatte *et al* [72] have investigated the depth-dependence of MTR values in
57 bovine cartilage samples and observed higher MTRs in the deep cartilage zone. This was attributed
58
59
60
61
62
63
64
65

1 to the depth-wise variation in cartilage collagen content as well as variations in the radial orientation of
2 collagen fibrils and variations in the bound water fraction throughout the thickness of the cartilage.
3 Yao *et al*[76] have reported on the insensitivity of MTR measurements to early degenerative changes
4 in cartilage, also suggesting that the dependence of the MTR on multiple factors makes variation in
5 MTRs difficult to interpret.
6
7
8
9

10 A recent development of the magnetisation transfer principle is the chemical exchange-dependent
11 saturation transfer (CEST) technique.[77] Exchangeable protons of a solute are selectively excited
12 and chemical exchange of these protons with water protons results in a detectable decrease in the
13 magnetisation of the bulk water pool[78] (Figure 6c). By saturating hydroxyl residues of
14 glycosaminoglycan (Figure 7), the CEST effect can be exploited to directly measure GAG content *in*
15 *vivo*. [79] In this study by Ling *et al*, the gagCEST technique was implemented *in vivo* on a 3 T clinical
16 scanner and was able to show the demarcation of a cartilage lesion in a human knee joint. Schmitt *et*
17 *al*[80] have compared the gagCEST technique with sodium MRI in a study performed at 7 T on
18 patients who had undergone cartilage repair surgery, with a high correlation observed between the
19 two techniques.
20
21
22
23
24
25
26
27
28
29
30
31
32
33
34

35 Diffusion MRI

36 Diffusion MRI techniques are sensitive to the restriction of motion of water molecules bound within a
37 macromolecular environment. Diffusion sensitive MRI methods use paired magnetic field gradient
38 pulses to probe the motion of nuclei in the direction of the applied magnetic field gradient.[81] The two
39 pulses are of equal duration and amplitude and are separated by a time delay (Δ). The net effect of
40 the paired gradient pulses is to dephase magnetisation from nuclei which have undergone diffusion
41 during the time delay resulting in a measurable signal attenuation. The measured signal (S), is related
42 to the diffusion coefficient (D) of the nuclei by the Stejskal-Tanner equation[82]
43
44
45
46
47
48
49
50
51

$$52 \frac{S}{S_0} = \exp(-\gamma^2 G^2 \delta^2 \left(\Delta - \frac{\delta}{3}\right) D) \quad (1)$$

53 where γ is the gyromagnetic ratio of the diffusing nuclei, G and δ are the amplitude and duration of the
54 applied gradient pulses respectively and S_0 is the measured signal intensity when $G=0$. Typically, a
55 diffusion sensitive MRI sequence consists of a number of diffusion gradient pulses applied along
56
57
58
59
60
61
62
63
64
65

1 multiple axes as well as imaging gradients for spatial localisation of the signal. It then becomes
2 convenient to summarise the combined influence of the gradients through calculation of the b-
3 factor.[83] The b-factor determines the overall diffusion-weighting of a sequence in the same way that
4 the echo time characterises the degree of T_2 -weighting. Acquisition of images with multiple b-factors
5 thus allows the diffusion coefficient to be mapped on a pixel-by-pixel basis.
6
7

8
9
10 When measuring the diffusion coefficient of water molecules in physiological systems, there is
11 significant interaction between the water molecules and their surrounding environment during the
12 timescale of the experiment and the parameter measured is the apparent diffusion coefficient (ADC).
13 Consequently, measuring the ADC of water molecules within the cartilage ECM can be used to infer
14 cartilage tissue structure and architecture,[84, 85] with increased diffusivity linked to structural
15 degradation of the ECM. The potential of diffusion weighted imaging (DWI) has been demonstrated as
16 a method for assessing cartilage degeneration *in vivo*[86] and monitoring its repair following
17 surgery.[8, 87] A recent longitudinal study by Friedrich *et al*[88] has shown the ability of DWI to
18 differentiate between healthy and repaired cartilage at different time points after surgery of patients
19 who underwent matrix-assisted autologous chondrocyte transplantation. The authors highlight the
20 difficulty of obtaining precise measures of the diffusion values, and compare only the relative changes
21 in diffusivity in this study.
22
23
24
25
26
27
28
29
30
31
32
33
34
35

36 Whereas DWI can report the localised average diffusivity, diffusion tensor imaging (DTI) can be used
37 to obtain the directionality of localised diffusion, revealing the orientation of collagen fibrils in the
38 cartilage ECM.[89] DTI has been used to study the effects of compression on the cartilage collagen
39 network,[90] and a recent study has reported on the use of ultra-high field (17.6 T) DTI to inform a
40 finite element simulation of cartilage deformation.[91] At present though, DTI is unlikely to be
41 applicable for *in vivo* assessment of cartilage due to the intensive data analysis required as well as
42 lengthy acquisition times even at high field strengths.
43
44
45
46
47
48
49
50
51
52
53

54 **Imaging of related musculoskeletal tissues**

55
56 The focus so far has been on imaging methods for the assessment of articular cartilage. However,
57 MRI has also been able to show the involvement of related joint structures in the early expression of
58 OA.[92, 93] In this study, high resolution MRI of the hand was carried out using standard clinical
59
60
61
62
63
64
65

1 protocols on a 1.5 T scanner and compared to histological sections of cadaveric joints. Abnormalities
2 in the collateral ligaments of the distal interphalangeal joint were observed adjacent to sites of bone
3 oedema, bone erosion and new bone formation. In some cases ligament abnormalities were seen in
4 joints without large scale loss of cartilage, showing that ligament abnormalities may precede
5 degenerative changes in cartilage in some cases of OA.
6
7
8
9

10 The structure of the enthesis organ (the complex arrangement of ligaments and tendons and their
11 interfaces with bone) and its involvement in both inflammatory and degenerative arthritides is also of
12 interest.[94, 95] The use of both conventional MR sequences and UTE sequences for visualisation of
13 the enthesis has been studied,[42, 96] allowing the presence of fibrocartilage to be shown in the
14 enthesis. Previously histological sectioning has been required to determine the presence of
15 fibrocartilage. Imaging sequences utilising ultra-short echo times or UTE sequences are a relatively
16 recent innovation in MRI.[97] Employing imaging sequences with echo times as short as 50 μ s allows
17 the signal components with very short T_2 relaxation times to be observed,[98] which otherwise decay
18 too rapidly to be observed with standard echo times (> 5 ms). UTE sequences have also enabled
19 magnetisation transfer contrast imaging of tissues with rapid signal decay; Springer *et al* [99] have
20 measured MTRs *in vitro* in bovine cortical bone and *in vivo* in healthy human volunteers,
21 demonstrating the feasibility of the technique for clinical applications.
22
23
24
25
26
27
28
29
30
31
32
33
34
35
36
37
38

39 **Key open questions**

40
41 There is currently significant interest in the identification of biomarkers that would allow the early
42 detection of osteoarthritis.[2] There are a number of MR measurable parameters that have been
43 shown to be sensitive to early biochemical changes, including depletion of GAG and collagen fibre
44 breakdown. The question remains as to which of these parameters are best suited to fulfil the needs
45 of clinicians in making an early diagnosis. For routine use in a clinical setting potential imaging
46 techniques should be reliably performed in a relatively short time. Long scanning sessions are
47 uncomfortable for patients and may result in poor quality images due to patient motion. If the ultimate
48 goal of routine screening of patient groups at risk of developing OA is to be achieved, then completely
49 non-invasive MR methods would be preferable; methods requiring intravenous administration of
50
51
52
53
54
55
56
57
58
59
60
61
62
63
64
65

1 contrast agents are not only invasive and associated with increased incidence of nephrogenic
2 fibrosing dermopathy but also prolong the examination period, reducing their practicality.
3

4 At present, MRI measures of cartilage composition in OA are predominantly used in a research
5 setting to assess potential treatment strategies and to better understand the disease process.
6 Ultimately, the wider clinical applicability of these techniques will depend on the development of new
7 OA treatments e.g. drugs, physiotherapy regimes or minimally invasive surgical procedures. In this
8 context, the ability to detect early cartilage changes (before the development of potentially irreversible
9 structural abnormalities) and assess disease progression and response to treatment would be of
10 potential clinical value. Another key issue for detecting early cartilage changes using MRI would be
11 targeting of appropriate patient groups at risk of developing OA. Such screening may be based on a
12 variety of predisposing factors including those associated with certain high risk occupations and
13 sporting activities as well as previous injury.
14
15
16
17
18
19
20
21
22
23
24

25 MRI methods that are sensitive to the GAG content of cartilage currently represent the most
26 promising opportunities for early non-invasive assessment of cartilage degeneration. Both sodium
27 imaging and dGEMRIC offer a highly specific method of GAG quantification through measurement of
28 tissue fixed charge density. However, the dGEMRIC method requires the use of exogenous contrast
29 agent making it subject to the disadvantages cited above. Sodium MRI is completely non-invasive but
30 the method is technically demanding, requiring specialist RF coils, pulse sequences and high field
31 strength magnets to obtain useful results. Development of the technique may be stimulated by the
32 increasing presence of clinical 3T scanners but it may be that even higher field strengths are required.
33
34
35
36
37
38
39
40
41
42

43 The specificity and non-invasiveness of the gagCEST technique would appear to make it a highly
44 favourable technique with which to assess GAG content *in vivo*. The feasibility of the technique for *in*
45 *vivo* studies has been demonstrated[79, 80] and the major challenge will be to develop robust CEST
46 pulse sequences suitable for use in a clinical setting.
47
48
49
50

51 The potential for $T_{1\rho}$ to provide a completely non-invasive, specific measure of cartilage PG content in
52 a clinically feasible time remains. Further studies on the specificity and sensitivity of the technique are
53 required as well the development and implementation of standardised pulse sequences. These
54 challenges appear to be surmountable in the short to medium term and, encouragingly, should be
55 achievable at current clinically available magnet field strengths.
56
57
58
59
60
61
62
63
64
65

1
2
3
4
5
6
7
8
9
10
11
12
13
14
15
16
17
18
19
20
21
22
23
24
25
26
27
28
29
30
31
32
33
34
35
36
37
38
39
40
41
42
43
44
45
46
47
48
49
50
51
52
53
54
55
56
57
58
59
60
61
62
63
64
65

With recent opinion suggesting that OA may initiate in the synovium, ligaments, tendons, menisci and other interrelated joint structures,[100, 101] the search for imaging biomarkers in these areas may represent an alternative approach to the diagnosis of early OA. Through this approach it may also be possible to obtain important information about the phenotypic expression of OA in general. The study by Tan *et al*[92] has shown that the early involvement of the collateral ligaments in hand OA can be observed using well developed MRI protocols and currently available equipment. The opportunity exists to translate this approach to other diarthrodial joints including the knee, although full joint coverage at sufficiently high resolution will be more challenging for larger joints. UTE sequences may also be beneficial for the purpose of delineating structures with very short T_2 relaxation times.

Closely related to the search for biomarkers of osteoarthritis, is the desire to infer the mechanical properties of cartilage using quantitative MRI. This would be of benefit to biotribological studies of articulating joints, allowing the effects of mechanical loading to be studied during *in vitro* wear simulations using dynamic MR sequences. The Finnish group at Kuopio/Oulu have contributed the majority of the research in this area and have developed a finite element model of cartilage based on its microscopic composition. Such models will benefit from input of the whole range of quantitative MR parameters discussed here. Much of the microscopic structure and composition of cartilage can be elucidated using MRI: collagen fibril orientation, PG and fluid content, however the depth-wise variation in collagen content is not yet quantifiable using MRI, and must be obtained using polarised light microscopy (PLM) or similar techniques.

Conclusions

Functional assessment of cartilage and other musculoskeletal tissues is possible through application of a number of quantitative MRI techniques. MR techniques exist that are sensitive to different aspects of the micro-anatomical structure of cartilage, including tissue hydration, glycosaminoglycan (GAG) content and the architecture of the cartilage collagen network.

Quantitative assessment of cartilage GAG content represents perhaps the best opportunity to identify cartilage degradation at its earliest point and there are several MR techniques suitable for this purpose. $T_{1\rho}$ measurement may prove to be the most clinically feasible if the sensitivity and specificity of the parameter for cartilage GAG content can be established. Both dGEMRIC and sodium MRI offer

1 highly specific measurement of GAG content through quantification of fixed charge density, though
2 their clinical implementation may be limited due to the invasiveness of the technique in the case of
3 dGEMRIC and hardware dependency in the case of sodium MRI. Further development of emerging
4 CEST-MR methods may allow for direct GAG quantification using the gagCEST technique.
5
6

7
8
9 Quantitative relaxometry of cartilage offers a less specific assessment of cartilage with native T_1 and
10 T_2 values as well as magnetisation transfer interactions dependent upon a variety of factors not
11 limited to water content and mobility, GAG content and collagen fibril orientation. Further
12 understanding of the macromolecular processes and interactions that determine tissue relaxation
13 times may allow these phenomenological parameters to be incorporated into computational models
14 able to predict the biomechanical properties of cartilage. Translating MRI parameters into specific
15 mechanical properties of musculoskeletal tissues represents a significant challenge, but the potential
16 benefits to areas of regenerative medicine and biomedical engineering of a means of non-invasive,
17 quantitative assessment are clear.
18
19
20
21
22
23
24
25
26
27
28
29
30
31
32
33
34
35
36
37
38
39
40
41
42
43
44
45
46
47
48
49
50
51
52
53
54
55
56
57
58
59
60
61
62
63
64
65

1
2
3 **Figure Legends**
4
5
6

7 **Figure 1 a) Macromolecular composition of cartilage. The collagen fibril network provides the**
8 **structural framework for cartilage and confers resistance to shear and tensile forces.**
9 **Proteoglycans are embedded within the collagen network and consist of a central protein core**
10 **and covalently attached negatively-charged glycosaminoglycan (GAG) side-chains. The**
11 **negatively-charged GAGs increase the local concentration of cationic species such as Na⁺ and**
12 **help to maintain fluid within the tissue, bestowing stiffness and resistance to compressive**
13 **forces. b) In proteoglycan depleted cartilage, the loss of negatively-charged GAGs and**
14 **corresponding reduction in mobile cation concentration diminish the ability of the cartilage**
15 **macromolecular matrix to constrain fluid, reducing its capacity to withstand compression.**
16
17
18
19
20
21
22
23
24
25
26
27
28
29
30
31

32 **Figure 2 Conventional parameter-weighted magnetic resonance images of a cadaveric knee**
33 **joint. a) 2-D coronal intermediate-weighted spin-echo image used to assess gross joint**
34 **alignment, collateral ligaments, medial and lateral menisci as well as cartilage morphology and**
35 **presence or absence of sub-chondral cysts. b) 3-D T_2^* -weighted gradient echo image with**
36 **selective water excitation; a 3-D acquisition which allows the cartilage thickness and volume**
37 **to be measured as well as providing information about bone attrition and osteophyte**
38 **formation.**
39
40
41
42
43
44
45
46
47
48
49

50 **Figure 3 Quantitative MR parameter mapping. A pixel-by-pixel map of a single MR property is**
51 **displayed on top of an anatomical image, showing the variation of that particular parameter in**
52 **a region of interest (ROI). This particular image shows the variation in T_2 relaxation time in the**
53 **femoral articular cartilage and patellar cartilage of the knee joint.**
54
55
56
57
58
59
60
61
62
63
64
65

1
2
3
4
5
6
7
8
9
10
11
12
13
14
15
16
17
18
19
20
21
22
23
24
25
26
27
28
29
30
31
32
33
34
35
36
37
38
39
40
41
42
43
44
45
46
47
48
49
50
51
52
53
54
55
56
57
58
59
60
61
62
63
64
65

Figure 4 Distribution of gadolinium diethylenetriamine pentaacetic acid ($[\text{Gd}(\text{DTPA})^2]$) in a) healthy and b) glycosaminoglycan (GAG) depleted cartilage extracellular matrix. The local concentration of the administered gadolinium contrast agent is inversely proportional to cartilage GAG content due to the electrostatic repulsion between negatively-charged GAGs and the negatively-charged contrast agent. Water proton T_1 relaxation times are reduced in the vicinity of the paramagnetic contrast agent and can therefore be used to measure GAG concentration.

Figure 5 Distribution of sodium ions (Na^+) in a) healthy and b) glycosaminoglycan (GAG) depleted cartilage extracellular matrix. The negative fixed charge density of glycosaminoglycan is balanced by cationic sodium ions. GAG depleted regions have lower negative fixed charge density and therefore fewer sodium ions. MRI techniques can measure the sodium concentration, allowing the fixed charge density and GAG concentration to be calculated.

Figure 6 Saturation transfer effects between protons in the free and bound water pools and exchangeable protons of solute molecules. a) In magnetisation transfer (MT), an off-resonance radio-frequency (RF) pulse saturates the broad proton resonance of low mobility bound water molecules. Proton exchange between bound water molecules and the free water pool results in saturation transfer to the free water pool and a detectable reduction in the signal intensity of the free water resonance (b). The magnetisation transfer ratio is defined as $\text{MTR} = 1 - S_{\text{MT}} / S_0$, where S_0 is the signal intensity recorded without a preparatory saturation pulse and S_{MT} is the signal intensity observed with the inclusion of a preparatory saturation pulse. c) In the chemical exchange saturation transfer (CEST) technique solute protons are selectively saturated using by an RF pulse. Chemical exchange of the solute protons with water protons again results in saturation transfer to the free water pool and a measurable reduction in water proton signal intensity.

Figure 7 Molecular structure of one disaccharide unit of chondroitin-4-sulfate, one of the constituent glycosaminoglycans of proteoglycan. Exchangeable protons that contribute to the chemical exchange saturation transfer (CEST) effects seen using the gagCEST technique are highlighted.

1
2
3
4
5
6
7
8
9
10
11
12
13
14
15
16
17
18
19
20
21
22
23
24
25
26
27
28
29
30
31
32
33
34
35
36
37
38
39
40
41
42
43
44
45
46
47
48
49
50
51
52
53
54
55
56
57
58
59
60
61
62
63
64
65

1. Burstein D, Gray ML. Is MRI fulfilling its promise for molecular imaging of cartilage in arthritis? *Osteoarthritis Cartilage* 2006 14:1087-90.
2. Williams F, Spector T. Biomarkers in osteoarthritis. *Arthritis Research & Therapy* 2008 10:101.
3. Buckwalter JA, Mankin HJ. Instructional Course Lectures, The American Academy of Orthopaedic Surgeons - Articular Cartilage. Part I: Tissue Design and Chondrocyte-Matrix Interactions*†. *J Bone Joint Surg Am* 1997 79:600-11.
4. Mow VC, Holmes MH, Michael Lai W. Fluid transport and mechanical properties of articular cartilage: A review. *Journal of Biomechanics* 1984 17:377-94.
5. Buckwalter JA, Mankin HJ. Instructional Course Lectures, The American Academy of Orthopaedic Surgeons - Articular Cartilage. Part II: Degeneration and Osteoarthrosis, Repair, Regeneration, and Transplantation*†. *J Bone Joint Surg Am* 1997 79:612-32.
6. Gold GE, Chen CA, Koo S, Hargreaves BA, Bangerter NK. Recent Advances in MRI of Articular Cartilage. *Am J Roentgenol* 2009 193:628-38.
7. Peterfy CG, Schneider E, Nevitt M. The osteoarthritis initiative: report on the design rationale for the magnetic resonance imaging protocol for the knee. *Osteoarthritis Cartilage* 2008 16:1433-41.
8. Trattnig S, Domayer S, Welsch G, Mosher T, Eckstein F. MR imaging of cartilage and its repair in the knee - a review. *Eur Radiol* 2009 19:1582-94.
9. Disler DG, Recht MP, McCauley TR. MR imaging of articular cartilage. *Skeletal Radiol* 2000 29:367-77.
10. Halstead J, Bergin D, Keenan AM, Madden J, McGonagle D. Ligament and Bone Pathologic Abnormalities More Frequent in Neuropathic Joint Disease in Comparison With Degenerative Arthritis of the Foot and Ankle Implications for Understanding Rapidly Progressive Joint Degeneration. *Arthritis Rheum* 2010 62:2353-8.
11. Hu X, Norris DG. Advances in high-field magnetic resonance imaging. *Annual Review of Biomedical Engineering* 2004 6:157-84.
12. Chan W, Lang P, Stevens M, Sack K, Majumdar S, Stoller D, et al. Osteoarthritis of the knee: comparison of radiography, CT, and MR imaging to assess extent and severity. *Am J Roentgenol* 1991 157:799-806.
13. Peterfy C, Kothari M. Imaging osteoarthritis: Magnetic resonance imaging versus x-ray. *Current Rheumatology Reports* 2006 8:16-21.
14. Levitt M. *Spin Dynamics: Basics of Nuclear Magnetic Resonance*. New York: Wiley; 2008.
15. Nissi MJ, Rieppo J, Toyras J, Laasanen MS, Kiviranta I, Nieminen MT, et al. Estimation of mechanical properties of articular cartilage with MRI - dGEMRIC, T₂ and T₁ imaging in different species with variable stages of maturation. *Osteoarthritis Cartilage* 2007 15:1141-8.
16. Julkunen P, Korhonen RK, Nissi MJ, Jurvelin JS. Mechanical characterization of articular cartilage by combining magnetic resonance imaging and finite-element analysis - a potential functional imaging technique. *Phys Med Biol* 2008 53:2425-38.
17. Wiener E, Pfirmann CWA, Hodler J. Spatial variation in T₁ of healthy human articular cartilage of the knee joint. *Br J Radiol* 2010 83:476-85.
18. Bashir A, Gray ML, Burstein D. Gd-DTPA²⁻ as a measure of cartilage degradation. *Magn Reson Med* 1996 36:665-73.
19. Bashir A, Gray ML, Boutin RD, Burstein D. Glycosaminoglycan in articular cartilage: in vivo assessment with delayed Gd(DTPA)(2-)-enhanced MR imaging. *Radiology* 1997 205:551-8.
20. Williams A, Sharma L, McKenzie CA, Prasad PV, Burstein D. Delayed gadolinium-enhanced magnetic resonance imaging of cartilage in knee osteoarthritis: Findings at different radiographic stages of disease and relationship to malalignment. *Arthritis Rheumatism* 2005 52:3528-35.
21. Pollard TCB, McNally EG, Wilson DC, Wilson DR, Madler B, Watson M, et al. Localized Cartilage Assessment with Three-Dimensional dGEMRIC in Asymptomatic Hips with Normal Morphology and Cam Deformity. *J Bone Joint Surg-Am Vol* 2010 92A:2557-69.
22. Burstein D, Velyvis J, Scott KT, Stock KW, Kim YJ, Jaramillo D, et al. Protocol issues for delayed Gd(DTPA)(2-)-enhanced MRI: (dGEMRIC) for clinical evaluation of articular cartilage. *Magn Reson Med* 2001 45:36-41.
23. Silvast TS, Kokkonen HT, Jurvelin JS, Quinn TM, Nieminen MT, Toyras J. Diffusion and near-equilibrium distribution of MRI and CT contrast agents in articular cartilage. *Phys Med Biol* 2009 54:6823-36.

24. Mauck RL, Hung CT, Ateshian GA. Modeling of neutral solute transport in a dynamically loaded porous permeable gel: Implications for articular cartilage biosynthesis and tissue engineering. *J Biomech Eng-Trans ASME* 2003 125:602-14.
25. Williams A, Mikulis B, Krishnan N, Gray M, McKenzie C, Burstein D. Suitability of T-1Gd as the "dGEMRIC Index" at 1.5T and 3.0T. *Magn Reson Med* 2007 58:830-4.
26. Li W, Du H, Scheidegger R, Wu Y, Prasad PV. Value of Precontrast T₁ for dGEMRIC of Native Articular Cartilage. *J Magn Reson Imaging* 2009 29:494-7.
27. Bittersohl B, Hosalkar HS, Kim YJ, Werlen S, Siebenrock KA, Mamisch TC. Delayed Gadolinium-Enhanced Magnetic Resonance Imaging (dGEMRIC) of Hip Joint Cartilage in Femoroacetabular Impingement (FAI): Are Pre- and Postcontrast Imaging Both Necessary? *Magn Reson Med* 2009 62:1362-7.
28. Trattnig S, Burstein D, Szomolanyi P, Pinker K, Welsch GH, Mamisch TC. T₁ (Gd) Gives Comparable Information as Delta T₁ Relaxation Rate in dGEMRIC Evaluation of Cartilage Repair Tissue. *Invest Radiol* 2009 44:598-602.
29. McKenzie CA, Williams A, Prasad PV, Burstein D. Three-dimensional delayed gadolinium-enhanced MRI of cartilage (dGEMRIC) at 1.5T and 3.0T. *J Magn Reson Imaging* 2006 24:928-33.
30. Kimelman T, Vu A, Storey P, McKenzie C, Burstein D, Prasad P. Three-dimensional T₁ mapping for dGEMRIC at 3.0 T using the Look Locker method. *Invest Radiol* 2006 41:198-203.
31. Sur S, Mamisch TC, Hughes T, Kim YJ. High Resolution Fast T₁ Mapping Technique for dGEMRIC. *J Magn Reson Imaging* 2009 30:896-900.
32. David-Vaudey E, Ghosh S, Ries M, Majumdar S. T₂ relaxation time measurements in osteoarthritis. *Magn Reson Imaging* 2004 22:673-82.
33. Taylor C, Carballido-Gamio J, Majumdar S, Li XJ. Comparison of quantitative imaging of cartilage for osteoarthritis: T₂, T₁ rho, dGEMRIC and contrast-enhanced computed tomography. *Magn Reson Imaging* 2009 27:779-84.
34. Dardzinski BJ, Mosher TJ, Li S, Van Slyke MA, Smith MB. Spatial variation of T₂ in human articular cartilage. *Radiology* 1997 205:546-50.
35. Dunn TC, Lu Y, Jin H, Ries MD, Majumdar S. T₂ Relaxation Time of Cartilage at MR Imaging: Comparison with Severity of Knee Osteoarthritis. *Radiology* 2004 232:592-8.
36. Stehling C, Liebl H, Krug R, Lane NE, Nevitt MC, Lynch J, et al. Patellar Cartilage: T₂ Values and Morphologic Abnormalities at 3.0-T MR Imaging in Relation to Physical Activity in Asymptomatic Subjects from the Osteoarthritis Initiative. *Radiology* 2010 254:509-20.
37. Xia Y. Relaxation anisotropy in cartilage by NMR microscopy (muMRI) at 14-mum resolution. *Magn Reson Med* 1998 39:941-9.
38. Xia Y, Moody JB, Alhadlaq H. Orientational dependence of T₂ relaxation in articular cartilage: A microscopic MRI (muMRI) study. *Magn Reson Med* 2002 48:460-9.
39. Nissi MJ, Rieppo J, Töyräs J, Laasanen MS, Kiviranta I, Jurvelin JS, et al. T₂ relaxation time mapping reveals age- and species-related diversity of collagen network architecture in articular cartilage. *Osteoarthritis Cartilage* 2006 14:1265-71.
40. Shapiro EM, Borthakur A, Kaufman JH, Leigh JS, Reddy R. Water distribution patterns inside bovine articular cartilage as visualized by ¹H magnetic resonance imaging. *Osteoarthritis Cartilage* 2001 9:533-8.
41. Wayne JS, Kraft KA, Shields KJ, Yin C, Owen JR, Disler DG. MR Imaging of Normal and Matrix-depleted Cartilage: Correlation with Biomechanical Function and Biochemical Composition. *Radiology* 2003 228:493-9.
42. Benjamin M, Milz S, Bydder GM. Magnetic resonance imaging of entheses. Part 1. *Clin Radiol* 2008 63:691-703.
43. Williams A, Qian Y, Bear D, Chu CR. Assessing degeneration of human articular cartilage with ultra-short echo time (UTE) T₂* mapping. *Osteoarthritis Cartilage* 2010 18:539-46.
44. Borthakur A, Mellon E, Niyogi S, Witschey W, Kneeland JB, Reddy R. Sodium and T₁rho MRI for molecular and diagnostic imaging of articular cartilage. *NMR in Biomedicine* 2006 19:781-821.
45. Duvvuri U, Reddy R, Patel SD, Kaufman JH, Kneeland JB, Leigh JS. T_{1ρ}-relaxation in articular cartilage: Effects of enzymatic degradation. *Magn Reson Med* 1997 38:863-7.
46. Pakin SK, Schweitzer ME, Regatte RR. 3D-T₁rho quantitation of patellar cartilage at 3.0T. *J Magn Reson Imaging* 2006 24:1357-63.
47. Li X, Han ET, Busse RF, Majumdar S. In vivo T₁rho mapping in cartilage using 3D magnetization-prepared angle-modulated partitioned k-space spoiled gradient echo snapshots (3D MAPSS). *Magn Reson Med* 2008 59:298-307.

48. Akella SVS, Regatte RR, Gougoutas AJ, Borthakur A, Shapiro EM, Kneeland JB, et al. Proteoglycan-induced changes in T_1 rho-relaxation of articular cartilage at 4T. *Magn Reson Med* 2001 46:419-23.
49. Witschey WRT, Borthakur A, Fenty M, Kneeland BJ, Lonner JH, Mc Ardle EL, et al. T_1 rho MRI quantification of arthroscopically confirmed cartilage degeneration. *Magn Reson Med* 2010 63:1376-82.
50. Holtzman DJ, Theologis AA, Carballido-Gamio J, Majumdar S, Li XJ, Benjamin C. T_1 rho and T-2 Quantitative Magnetic Resonance Imaging Analysis of Cartilage Regeneration Following Microfracture and Mosaicplasty Cartilage Resurfacing Procedures. *J Magn Reson Imaging* 2010 32:914-23.
51. Li X, Benjamin Ma C, Link TM, Castillo DD, Blumenkrantz G, Lozano J, et al. In vivo T_1 [rho] and T_2 mapping of articular cartilage in osteoarthritis of the knee using 3 T MRI. *Osteoarthritis Cartilage* 2007 15:789-97.
52. Regatte RR, Akella SVS, Borthakur A, Kneeland JB, Reddy R. Proteoglycan Depletion-Induced Changes in Transverse Relaxation Maps of Cartilage: Comparison of T_2 and T_1 [rho]. *Acad Radiol* 2002 9:1388-94.
53. Regatte RR, Akella SVS, Lonner JH, Kneeland JB, Reddy R. T_1 rho relaxation mapping in human osteoarthritis (OA) cartilage: Comparison of T_1 rho with T_2 . *J Magn Reson Imaging* 2006 23:547-53.
54. Akella SVS, Regatte RR, Wheaton AJ, Borthakur A, Reddy R. Reduction of residual dipolar interaction in cartilage by spin-lock technique. *Magn Reson Med* 2004 52:1103-9.
55. Menezes NM, Gray ML, Hartke JR, Burstein D. T_2 and T_1 rho MRI in articular cartilage systems. *Magn Reson Med* 2004 51:503-9.
56. Schick F. Whole-body MRI at high field: technical limits and clinical potential. *Eur Radiol* 2005 15:946-59.
57. Katta J, Jin Z, Ingham E, Fisher J. Biotribology of articular cartilage--A review of the recent advances. *Med Eng Phys* 2008 30:1349-63.
58. Kleemann RU, Krockner D, Cedraro A, Tuischer J, Duda GN. Altered cartilage mechanics and histology in knee osteoarthritis: relation to clinical assessment (ICRS Grade). *Osteoarthritis Cartilage* 2005 13:958-63.
59. Juras V, Bittsansky M, Majdisova Z, Szomolanyi P, Sulzbacher I, Gabler S, et al. In vitro determination of biomechanical properties of human articular cartilage in osteoarthritis using multi-parametric MRI. *J Magn Reson* 2009 197:40-7.
60. Wheaton AJ, Dodge GR, Elliott DM, Nicoll SB, Reddy R. Quantification of cartilage biomechanical and biochemical properties via $T_{1\rho}$ magnetic resonance imaging. *Magn Reson Med* 2005 54:1087-93.
61. Saarakkala S, Julkunen P, Kiviranta P, Mäkitalo J, Jurvelin JS, Korhonen RK. Depth-wise progression of osteoarthritis in human articular cartilage: investigation of composition, structure and biomechanics. *Osteoarthritis Cartilage* 2010 18:73-81.
62. Granot J. Sodium imaging of human body organs and extremities in vivo. *Radiology* 1988 167:547-50.
63. Grobner T. Gadolinium – a specific trigger for the development of nephrogenic fibrosing dermopathy and nephrogenic systemic fibrosis? *Nephrol Dial Transplant* 2006 21:1104-8.
64. Reddy R, Insko EK, Noyszewski EA, Dandora R, Kneeland JB, Leigh JS. Sodium MRI of human articular cartilage in vivo. *Magn Reson Med* 1998 39:697-701.
65. Borthakur A, Shapiro EM, Beers J, Kudchodkar S, Kneeland JB, Reddy R. Sensitivity of MRI to proteoglycan depletion in cartilage: comparison of sodium and proton MRI. *Osteoarthritis Cartilage* 2000 8:288-93.
66. Shapiro EM, Borthakur A, Gougoutas A, Reddy R. ^{23}Na MRI accurately measures fixed charge density in articular cartilage. *Magn Reson Med* 2002 47:284-91.
67. Robson MD, Gatehouse PD, Bydder M, Bydder GM. Magnetic resonance: An introduction to ultrashort TE (UTE) imaging. *J Comput Assist Tomogr* 2003 27:825-46.
68. Nielles-Vallespin S, Weber M-A, Bock M, Bongers A, Speier P, Combs SE, et al. 3D radial projection technique with ultrashort echo times for sodium MRI: Clinical applications in human brain and skeletal muscle. *Magn Reson Med* 2007 57:74-81.
69. Wang LG, Wu Y, Chang G, Oesingmann N, Schweitzer ME, Jerschow A, et al. Rapid Isotropic 3D-Sodium MRI of the Knee Joint In Vivo at 7T. *J Magn Reson Imaging* 2009 30:606-14.
70. Wolff SD, Balaban RS. Magnetization transfer contrast (MTC) and tissue water proton relaxation in vivo. *Magn Reson Med* 1989 10:135-44.

71. Lin P-C, Reiter DA, Spencer RG. Sensitivity and specificity of univariate MRI analysis of experimentally degraded cartilage. *Magn Reson Med* 2009 62:1311-8.
72. Regatte RR, Akella SVS, Reddy R. Depth-dependent proton magnetization transfer in articular cartilage. *J Magn Reson Imaging* 2005 22:318-23.
73. Gray ML, Burstein D, Lesperance LM, Gehrke L. Magnetization transfer in cartilage and its constituent macromolecules. *Magn Reson Med* 1995 34:319-25.
74. Wachsmuth L, Juretschke HP, Raiss RX. Can magnetization transfer magnetic resonance imaging follow proteoglycan depletion in articular cartilage? *Magnetic Resonance Materials in Physics Biology and Medicine* 1997 5:71-8.
75. Li W, Hong L, Hu L, Magin RL. Magnetization transfer imaging provides a quantitative measure of chondrogenic differentiation and tissue development. *Tissue Eng Part C Methods* 2010 16:1407-15.
76. Yao WW, Qu N, Lu ZH, Yang SX. The application of T₁ and T₂ relaxation time and magnetization transfer ratios to the early diagnosis of patellar cartilage osteoarthritis. *Skeletal Radiol* 2009 38:1055-62.
77. van Zijl PCM, Yadav NN. Chemical exchange saturation transfer (CEST): What is in a name and what isn't? *Magn Reson Med* 2011 65:927-48.
78. Ward KM, Aletras AH, Balaban RS. A New Class of Contrast Agents for MRI Based on Proton Chemical Exchange Dependent Saturation Transfer (CEST). *J Magn Reson* 2000 143:79-87.
79. Ling W, Regatte RR, Navon G, Jerschow A. Assessment of glycosaminoglycan concentration in vivo by chemical exchange-dependent saturation transfer (gagCEST). *Proc Natl Acad Sci* 2008 105:2266-70.
80. Schmitt B, Zbýň Š, Stelzeneder D, Jellus V, Paul D, Lauer L, et al. Cartilage Quality Assessment by Using Glycosaminoglycan Chemical Exchange Saturation Transfer and ²³Na MR Imaging at 7 T. *Radiology* 2011 260:257-64.
81. Freeman R. *Magnetic Resonance in Chemistry and Medicine*. Oxford: Oxford University Press; 2003.
82. Stejskal EO, Tanner JE. Spin diffusion measurements: spin echoes in the presence of a time-dependent field gradient. *J Chem Phys* 1965 42:288-92.
83. Mattiello J, Basser PJ, Lebihan D. Analytical expressions for the b-matrix in NMR diffusion imaging and spectroscopy. *J Magn Reson Ser A* 1994 108:131-41.
84. Burstein D, Gray ML, Hartman AL, Gipe R, Foy BD. Diffusion of small solutes in cartilage as measured by nuclear magnetic resonance (NMR) spectroscopy and imaging. *J Orthop Res* 1993 11:465-78.
85. Mlynárik V, Sulzbacher I, Bittšanský M, Fuiko R, Trattnig S. Investigation of apparent diffusion constant as an indicator of early degenerative disease in articular cartilage. *J Magn Reson Imaging* 2003 17:440-4.
86. Miller KL, Hargreaves BA, Gold GE, Pauly JM. Steady-state diffusion-weighted imaging of in vivo knee cartilage. *Magn Reson Med* 2004 51:394-8.
87. Mamisch TC, Menzel MI, Welsch GH, Bittersohl B, Salomonowitz E, Szomolanyi P, et al. Steady-state diffusion imaging for MR in-vivo evaluation of reparative cartilage after matrix-associated autologous chondrocyte transplantation at 3 tesla - Preliminary results. *Eur J Radiol* 2008 65:72-9.
88. Friedrich KM, Mamisch TC, Plank C, Langs G, Marlovits S, Salomonowitz E, et al. Diffusion-weighted imaging for the follow-up of patients after matrix-associated autologous chondrocyte transplantation. *Eur J Radiol* 2010 73:622-8.
89. Meder R, de Visser SK, Bowden JC, Bostrom T, Pope JM. Diffusion tensor imaging of articular cartilage as a measure of tissue microstructure. *Osteoarthritis Cartilage* 2006 14:875-81.
90. de Visser SK, Crawford RW, Pope JM. Structural adaptations in compressed articular cartilage measured by diffusion tensor imaging. *Osteoarthritis Cartilage* 2008 16:83-9.
91. Pierce DM, Trobin W, Raya JG, Trattnig S, Bischof H, Glaser C, et al. DT-MRI Based Computation of Collagen Fiber Deformation in Human Articular Cartilage: A Feasibility Study. *Ann Biomed Eng* 2010 38:2447-63.
92. Tan AL, Toumi H, Benjamin M, Grainger AJ, Tanner SF, Emery P, et al. Combined high-resolution magnetic resonance imaging and histological examination to explore the role of ligaments and tendons in the phenotypic expression of early hand osteoarthritis. *Ann Rheum Dis* 2006 65:1267-72.
93. Tan AL, Grainger AJ, Tanner SF, Shelley DM, Pease C, Emery P, et al. High-resolution magnetic resonance imaging for the assessment of hand osteoarthritis. *Arthritis Rheumatism* 2005 52:2355-65.

- 1 94. Benjamin M, Bydder GM. Magnetic resonance imaging of entheses using ultrashort TE (UTE)
2 pulse sequences. *J Magn Reson Imaging* 2007 25:381-9.
- 3 95. Benjamin M, McGonagle D. Histopathologic changes at "synovio–enthesal complexes"
4 suggesting a novel mechanism for synovitis in osteoarthritis and spondylarthritis. *Arthritis*
5 *Rheumatism* 2007 56:3601-9.
- 6 96. Benjamin M, Milz S, Bydder GM. Magnetic resonance imaging of entheses. Part 2. *Clin*
7 *Radiol* 2008 63:704-11.
- 8 97. Blamire AM. The technology of MRI -- the next 10 years? *Br J Radiol* 2008 81:601-17.
- 9 98. Gatehouse PD, Bydder GM. Magnetic Resonance Imaging of Short T₂ Components in Tissue.
10 *Clin Radiol* 2003 58:1-19.
- 11 99. Springer F, Martirosian P, Machann J, Schwenzer NF, Claussen CD, Schick F. Magnetization
12 Transfer Contrast Imaging in Bovine and Human Cortical Bone Applying an Ultrashort Echo Time
13 Sequence at 3 Tesla. *Magn Reson Med* 2009 61:1040-8.
- 14 100. McGonagle D, Tan AL, Carey J, Benjamin M. The anatomical basis for a novel classification
15 of osteoarthritis and allied disorders. *J Anat* 2010 216:279-91.
- 16 101. Brandt KD, Radin EL, Dieppe PA, van de Putte L. Yet more evidence that osteoarthritis is not
17 a cartilage disease. *Ann Rheum Dis* 2006 65:1261-4.
- 18
19
20
21
22
23
24
25
26
27
28
29
30
31
32
33
34
35
36
37
38
39
40
41
42
43
44
45
46
47
48
49
50
51
52
53
54
55
56
57
58
59
60
61
62
63
64
65

Figure_1

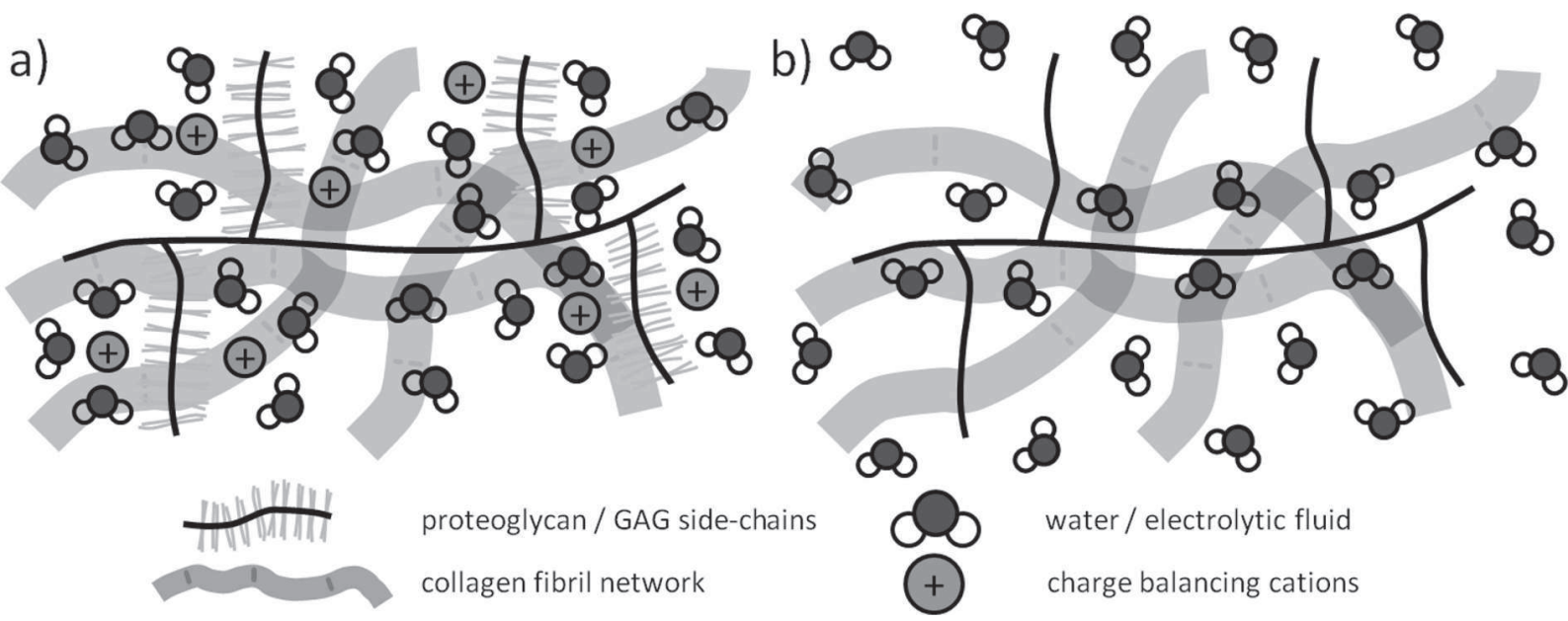


Figure_2
[Click here to download high resolution image](#)

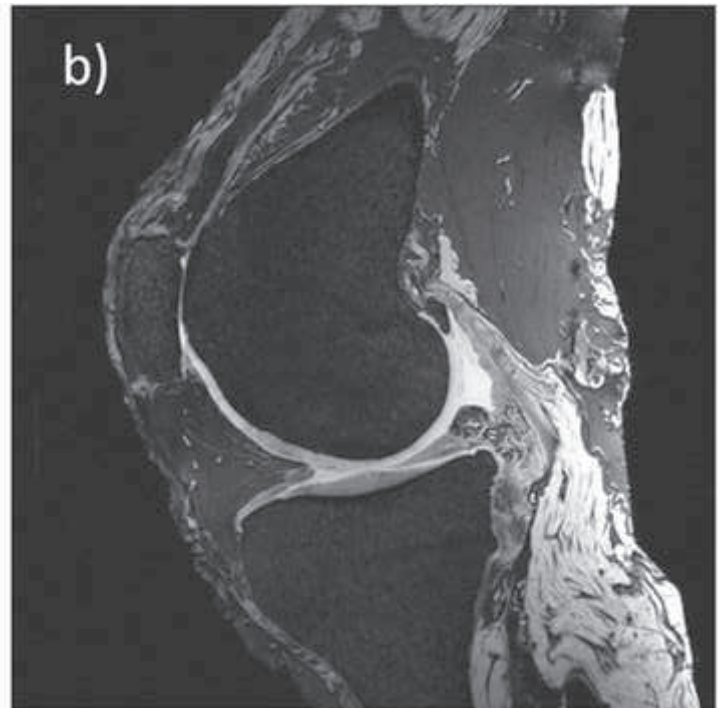


Figure_4

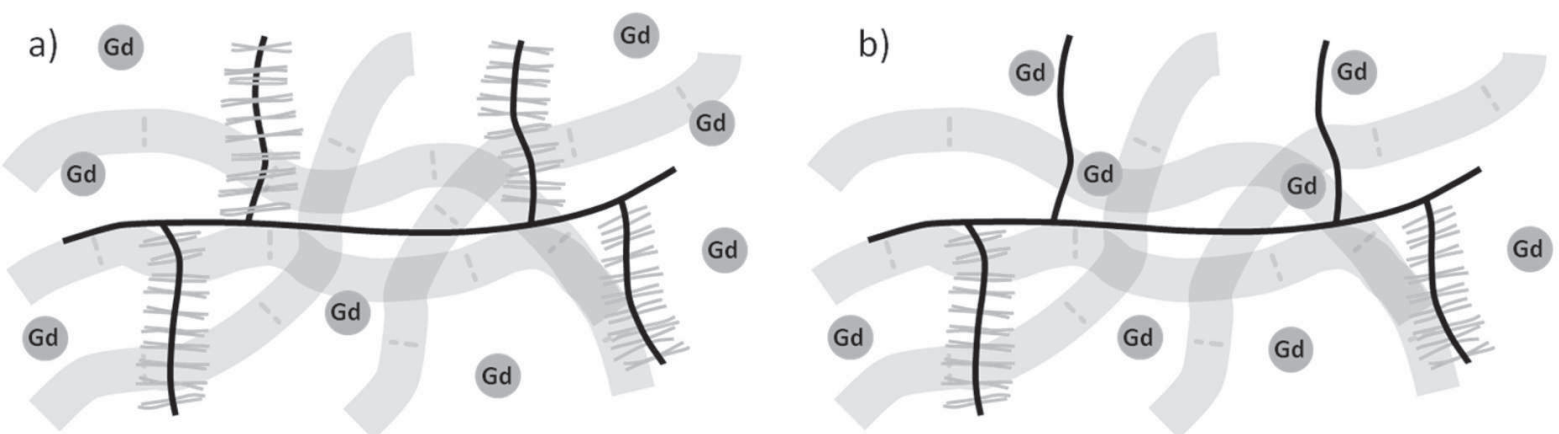


Figure_5

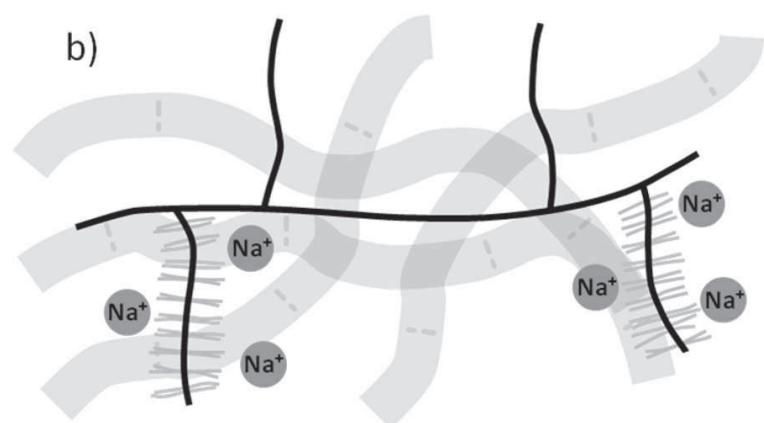
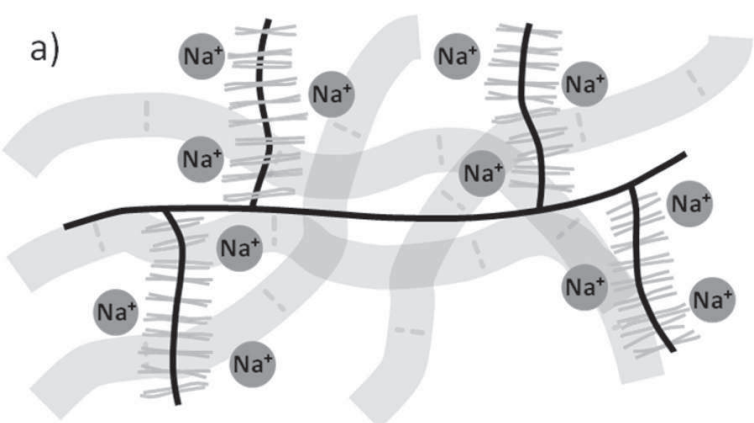


Figure_6

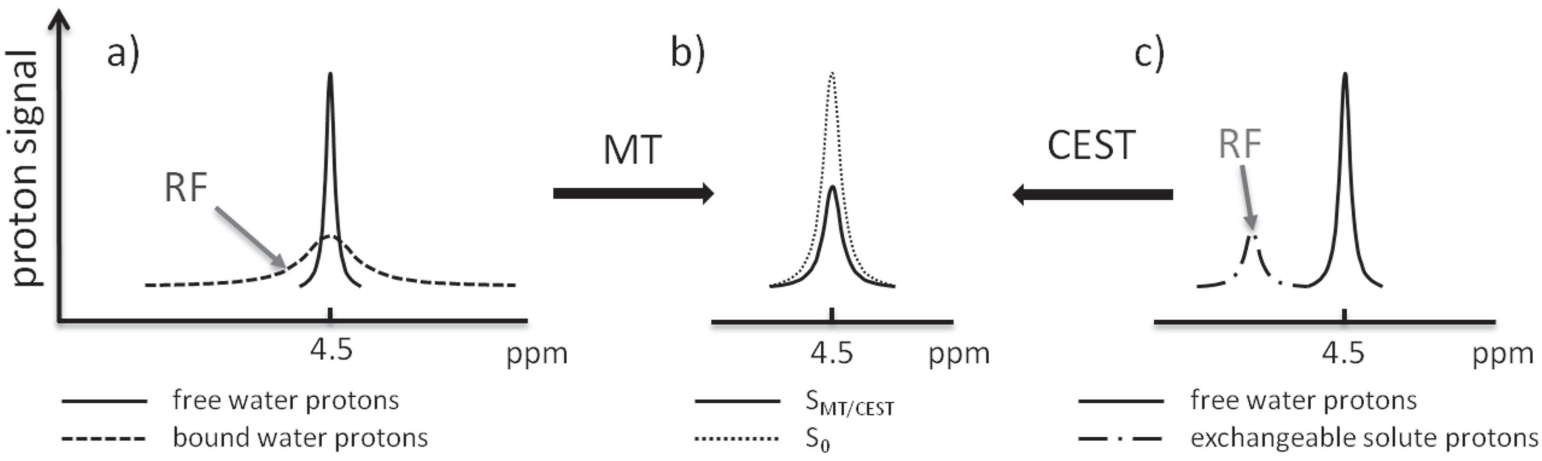


Figure_7

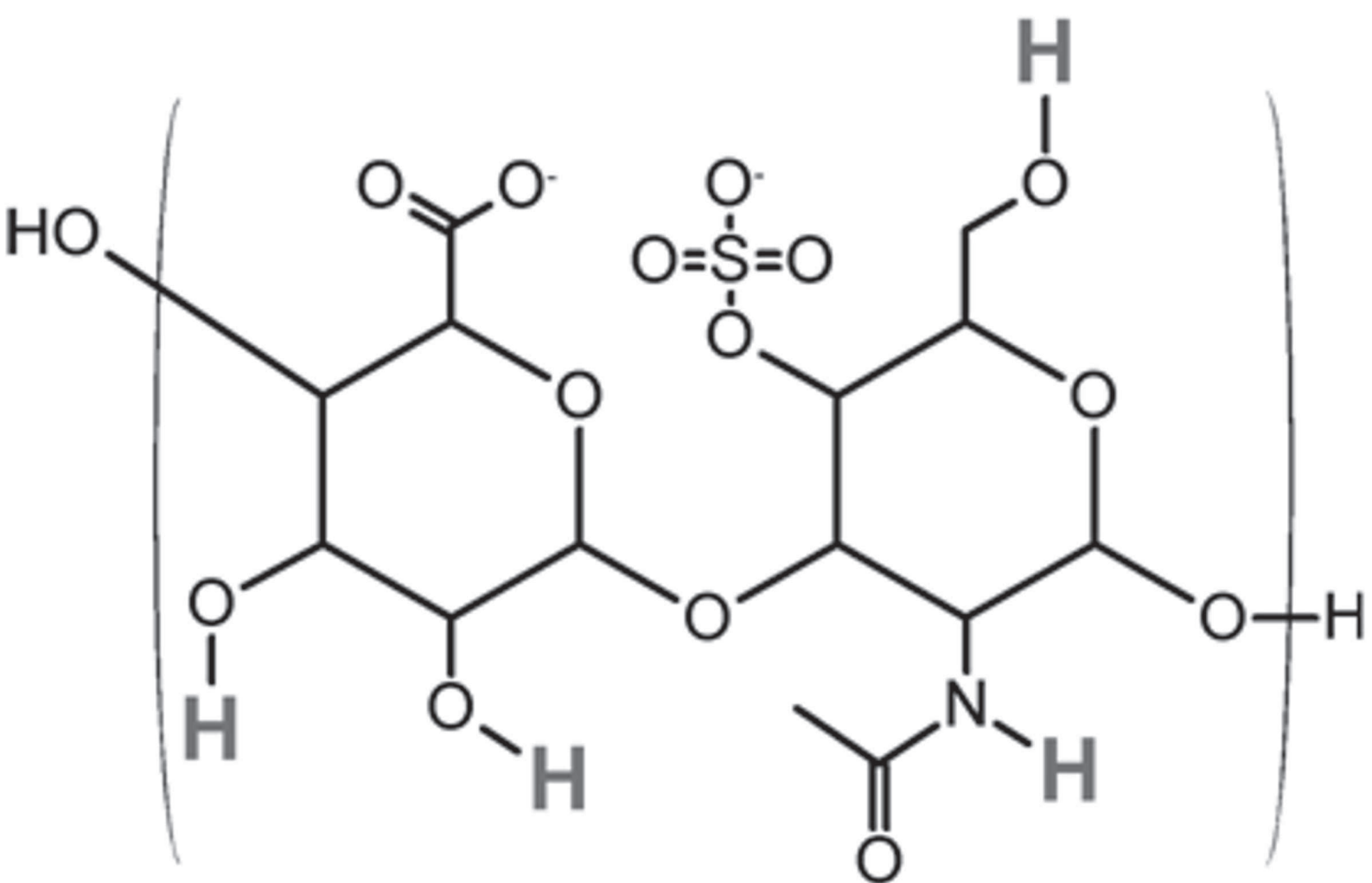
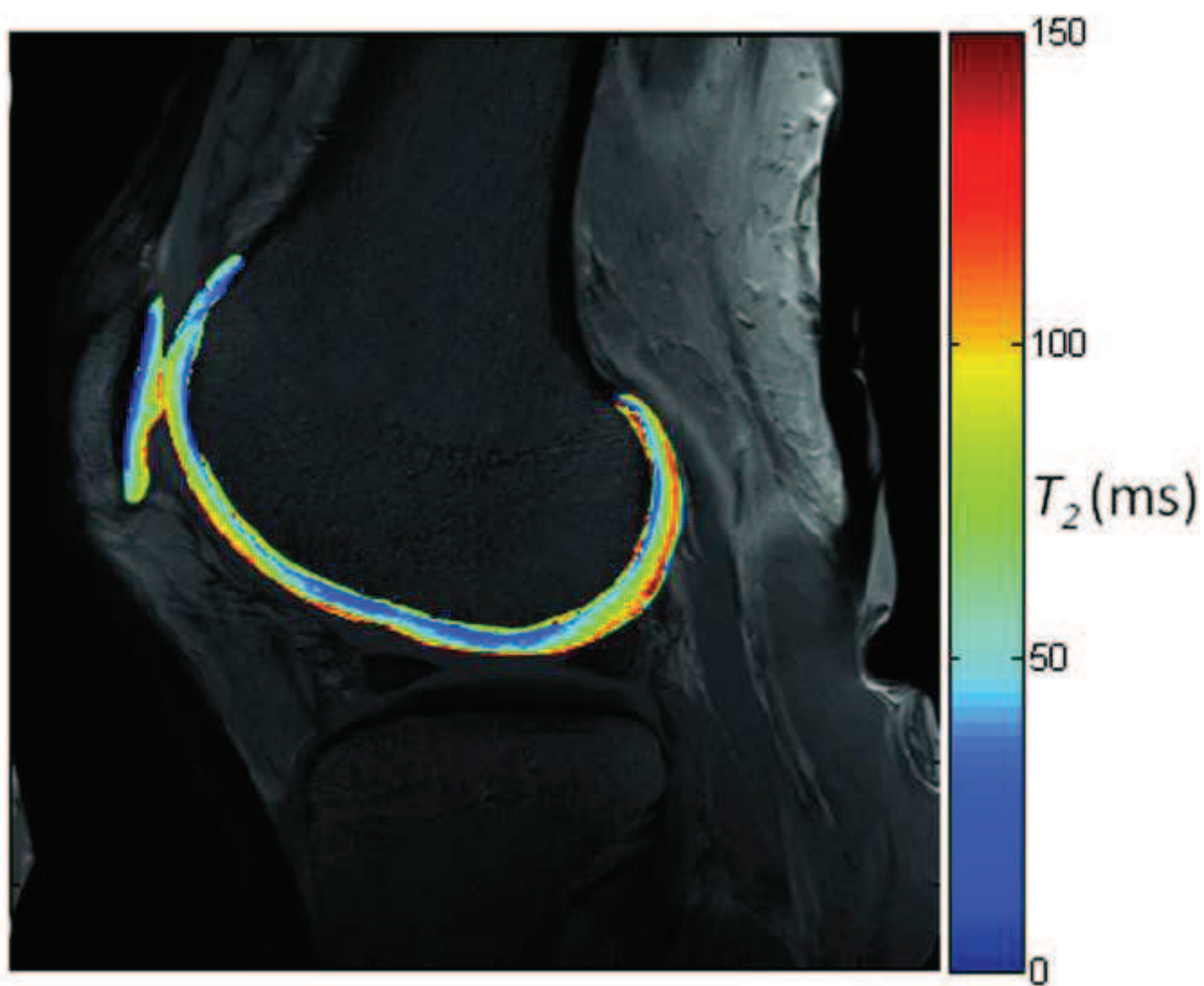


Figure_3
[Click here to download high resolution image](#)



*BJR Publishing Agreement

This piece of the submission is being sent via mail.